Journal of Animal Ecology
April 2022, Volume 91, Issue 4, Pages 805-818
https://doi.org/10.1111/1365-2656.13662
https://archimer.ifremer.fr/doc/00750/86228/

Seaweeds influence oyster microbiota and disease susceptibility

Dugeny Elyne [1], de Lorgeril Julien [2], Petton Bruno [1], Toulza Eve [2], Gueguen Yannick [2], Pernet Fabrice [1, *]

[1] Université de Brest, Ifremer, CNRS, IRD, LEMAR Plouzané, France
[2] IHPE, Université de Montpellier, CNRS, Ifremer, Université de Perpignan Via Domitia Montpellier ,France

* Corresponding author : Fabrice Pernet, email address : fabrice.pernet@ifremer.fr

Abstract :

1. A growing awareness of role that microbiota can play in mediating the effects of pathogens on hosts has given rise to the concept of the pathobiome. Recently, we demonstrated that the Pacific oyster mortality syndrome affecting Crassostrea gigas oysters is caused by infection with the Ostreid herpesvirus type 1 (OsHV-1) followed by infection with multiple bacterial taxa.

2. Here we extend the concept of this pathobiome beyond the host species and its bacterial microbiota by investigating how seaweed living in association with oysters influences their response to the disease. We hypothesized that by their mere presence in the environment, different species of seaweeds can positively or negatively influence the risk of disease in oysters by shaping their bacterial microbiota and their immune response. Although seaweed and oysters do not have direct ecological interactions, they are connected by seawater and likely share microbes.

3. To test our hypothesis, oysters were acclimated with green, brown or red algae for 2 weeks and then challenged with OsHV-1. We monitored host survival and pathogen proliferation and performed bacterial microbiota and transcriptome analyses.

4. We found that seaweeds can alter the bacterial microbiota of the host and its response to the disease. More particularly, green algae belonging to the genus Ulva spp. induced bacterial microbiota dysbiosis in oyster and modification of its transcriptional immune response leading to increased susceptibility to the disease.

5. This work provides a better understanding of a marine disease and highlights the importance of considering both macrobiotic and microbiotic interactions for conservation, management and exploitation of marine ecosystems and resources.

Keywords : bivalve, disease ecology, epidemiology, macroalgae, microbiome, pathogen

1. Introduction

Pathology has traditionally focused on single host-single pathogen interactions under given environmental conditions (Vayssier-Taussat *et al.* 2014; Ben-Horin *et al.* 2015; Cory & Deschodt 2017). However, invertebrate host and their pathogens are rarely found in isolation in natural situations. They indeed both exist within diverse and complex ecological communities, and interactions can influence the transmission and the impact of pathogens. Even where a primary agent can be identified, its effect is often influenced by other species interacting with the host, the pathogen or both (Vayssier-Taussat *et al.* 2014; Sweet & Bulling 2017; Bass *et al.* 2019; Byers 2020). More particularly, the microbiome, broadly defined as a collection of microorganisms living with the host (including bacteria, archaea, viruses, fungi, and unicellular eukaryotes), is increasingly recognized as a factor modifying interactions with pathogens. The pathobiome concept breaks down the idea of one pathogen = one disease, and highlights the role of the microbiome in pathogenesis (Vayssier-Taussat *et al.* 2014; Sweet & Bulling 2017; Bass *et al.* 2019).

In aquatic ecosystems, microorganisms from one host species can be released into the water column, transported by currents and thus colonize neighboring hosts of various species. Thus, all hosts in the same system can exchange microorganisms horizontally via the water column, and the concept of pathobiome can be extended to all ecosystem components including the sediment (Bass *et al.* 2019). Disruption of the microbial profile within the host caused by pathogen infection, physiological status, population density, or environmental perturbations, can potentially lead to a pathobiotic state.

A well-known case which illustrates the concept of pathobiome is the Pacific oyster mortality syndrome (POMS). POMS emerged in 2008, causing massive mortality in juvenile oysters, and

rapidly became panzootic (Pernet *et al.* 2016). Infection by Ostreid Herpesvirus type 1 µVar (OsHV-1 µvar) is the first critical step in the infectious process, leading to an immunocompromised state by altering hemocyte physiology (de Lorgeril *et al.* 2018). The viral infection is followed by dysbiosis, an imbalance in the host microbial community that is associated with disease. Dysbiosis leads to a secondary colonization by opportunistic bacterial pathogens and oyster death. The reshuffling of the oyster microbiota is an integral part of the infectious process induced by OsHV-1 (Lucasson *et al.* 2020). In addition, oysters with differing levels of resistance to POMS exhibit constitutive differences in their bacterial microbiota, suggesting that it might play a role in host immunity (King *et al.* 2019; Pathirana *et al.* 2019; Clerissi *et al.* 2020). More broadly, the oyster microbiome varies according to tissues, geographical location, food regime, temperature, infection or antibiotic use (Wegner *et al.* 2013; Lokmer & Wegner 2015; Lokmer *et al.* 2016; King *et al.* 2019; Clerissi *et al.* 2020; Dupont *et al.* 2020).

The risk of OsHV-1 mortality differs depending on the species that live around the oysters (Pernet *et al.* 2014; Pernet *et al.* 2021). Mortality risk of oysters held in mussel farms is lower than in oyster farms or empty farms, suggesting that mussels reduce the infection pressure on the host (Pernet *et al.* 2014). It is also possible that species that live around the oysters harbor species-specific bacterial microflora that influence the host microbiota, its immune response and its susceptibility to POMS (Pernet *et al.* 2021). The oyster pathobiome may be extended beyond the host species and its microbiota, leading to community models in which co-occurring species influences the health of the host population.

In this paper, we hypothesized that by their mere presence in the environment, different species of seaweeds can positively or negatively influence the risk of disease in oysters by shaping their bacterial microbiota and their immune response. Although seaweed and oysters

do not have direct ecological interactions such as competitive, predatory, or symbiotic relationships, they are connected by seawater and likely share microbes. Seaweed indeed harbor a rich diversity of associated bacteria (Egan *et al.* 2013) and their presence influence disease resistance of co-cultured shrimps (Anaya-Rosas *et al.* 2019). Here we developed a general study framework which include the oyster, its pathogen and bacterial microbiota, and seaweeds that can be applied to any other aquatic host.

To test our hypothesis, we exposed oysters to green (*Ulva* spp.), brown (*Fucus vesiculosus*) or red algae (*Solieria chordalis*) under laboratory conditions for two weeks and challenged them with OsHV-1. We chose these seaweeds because they thrive in different habitats and their bacterial microbiota was expected to be different (Lachnit *et al.* 2011; Singh & Reddy 2014). We monitored host survival and pathogen proliferation and we conducted bacterial microbiota and transcriptome analyses.

2. Material and methods

(a) Living organisms

Specific Pathogen Free (SPF) Pacific oysters *Crassostrea gigas* were produced under controlled conditions (Petton *et al.* 2015a; Le Roux *et al.* 2016). Briefly, adult oysters were collected in the wild in Fouras (Marennes-Oléron, France; 46°0’43’’ N, 1°7’3’’W) and moved to a grow-out farm located at Aber Benoît (northern Brittany, France; 48°34’30’’ N, 4°36’18’’W) until being used as broodstock. In January 2018, they were transferred at the Ifremer marine station located at Argenton (Brittany, France; 48°31’16’’N, 4°46’2’’W, France) in 500-L flow-through tanks at 17°C and fed *ad libitum* for 6 weeks for conditioning. Gametes from 76 females and 12 males were collected by stripping and fertilized on 20 February 2018 as previously described (Petton *et al.* 2015a). The oyster larvae were raised for 15 days at 25°C in 5 L

cylindrical tubes and settled on clutch for 10 d. The resulting spat were then transferred on 5 April 2018, at the Ifremer marine station located at Bouin (France) for nursery. They were then transferred back to the Ifremer facilities at the Argenton experimental site at 4 months-old, for the start of the experiment on 6 July 2018. The oysters were screened using an OsHV-1-specific quantitative PCR assay at the different stages of production and no OsHV-1 DNA was detected.

Before the experiment, oysters were maintained at 21°C in 500 L flow-through tanks, supplied with seawater filtered to 5µm and exposed to UV irradiation. Animals were fed constantly with a mixture of two phytoplankton species, the diatom *Chaetoceros muelleri* (CCAP 1010/3) and the Prymnesiophyceae *Tisochrysis lutea* (CCAP 927/14) (1:1 in dry weight). Food concentration was measured daily using an electronic particle counter (Coulter Multisizer 3) equipped with a 100 µm aperture tube and maintained at *ca*. 1500 μm^3 μL^{-1} in seawater at the outlet of the tanks. Temperature (21°C), salinity (34-35 g L^{-1}), pH_{NBS} (*ca*. 8.0) and oxygen (*ca*. 100%) were daily controlled with the WTW probes xi3101, cond340, pH3310 and FDO 925, respectively (Fisher scientific, Illkirch-Graffenstaden, France).

Seaweeds were collected on 5 July 2018 in the bay of Brest at Anse du Roz (48°19'21.7"N, 4°19'07.9"W) while seawater temperature was *ca.* 15.0°C. We retrieved the green algae *Ulva spp.* (Ulvophyceae), the brown algae *Fucus vesiculosus* (Phaeophyceae) and the red algae *Solieria chordalis* (Rhodophyceae). While *F. vesiculosus* and *S. chordalis* are easily visually identifiable species, this is not the case for *Ulva* spp. which exhibit multiple phenotypes and require DNA sequencing. As we have not performed any molecular analysis, identification of *Ulva* is limited to genus. These seaweeds were chosen because they thrive in different habitats, more or less anthropized, and their bacterial microbiota was expected to be different

(Lachnit *et al.* 2011; Singh & Reddy 2014). The green and the brown algae thrive in the middle shore of the intertidal zone and were collected by foot while the red algae are from the upper sublittoral level and were collected by scuba-diving. The proliferation of green algae is generally associated with eutrophication, i.e. nutrient enrichment beyond the self-regulatory capacity of the marine ecosystem. In Brittany, since the 70s, green algae outbreak every year late spring or early summer (Morand & Merceron 2005). The red algae *S. chordalis* is often found in healthy sheltered areas in calm waters, attached to a variety of substrates including gravel, shells and other algae. In the bay of Brest, *S. chordalis* is found in locally protected areas and in association with maërl bed (Floc'h *et al.* 1987). Finally, *Fucus vesiculosus* naturally live in zone of high water of neap tides (Hily & Jean 1997). Green and brown algae species naturally coexist with oysters while the red algae species is found nearby in deeper areas.

Seaweeds were collected attached to their substrata (stones, shells or pieces of maërl) and maintained alive during the entire duration of the experiment. Once in the laboratory, each group of seaweed and their associated microorganisms were kept separated in three 500 L flow-through tanks after rinsing with seawater, until the onset of the experiment.

(b) Experimental design

Here we used an open-flow system developed in a previous study (Pernet *et al.* 2021) (Fig. 1A). Virus-contaminated seawater enriched with phytoplankton was evenly distributed to 12 experimental units, each consisting of one header tank containing the seaweeds (green, brown or red algae) or left empty as control connected to one holding tank containing the SPF oysters (Fig. 1A). Each experimental unit was run in triplicate. Each header tank was connected to the seawater supply, to the food supply and to the source of infection by flexible tubes fitted inside a peristaltic pump. The seawater flow was set at 300 mL min^{-1} at the entry of each

header tank. Seawater overflowed from the header tank to the recipient tank. All the tanks were 45 L (60 x 40 x 19 cm) and illuminated by LED (EHEIM powerLED+, Deizisau, Germany) covering the full spectrum of sunlight to support the growth of algae. The photoperiod was fixed at 14L/10D. Seawater was homogenized by means of a recirculation pump and air bubbling to maintain O_2 level in all tanks. The phytoplankton concentration was adjusted at the inlet of the header tank containing the seaweed (or control) to obtain ~800 μm^3 μl^{-1} at the outlet of the holding tank (level 3). Seawater was sampled daily at the inlet and outlet of each holding tank to determine phytoplankton consumption using the electronic particle counter. The experiment consisted of two successive phases: acclimation and virus exposure (Fig. 1B).

Acclimation phase

Seaweed and recipient oysters were placed in header tanks and holding tanks respectively on July 6th 2018 (Fig. 1). The seaweeds were well interspersed throughout the available volume of the tank. We put equivalent volume of algae for each species, corresponding to about 600 g wet weight of brown and green algae, and 1000 g wet weight of red algae. The biomass of oysters was *ca*. 170 g ± 0.1 in each tank, corresponding to 340 individuals. Acclimation lasted for 14 d until 20 July 2018.

Virus exposure

The SPF oysters for injection were myorelaxed in $MgCl_2$ (50 g L^{-1} in a mixture of seawater and distilled water 40/60 v/v) at 21°C (Suquet *et al.* 2009) on July 19th 2018. A total of *ca*. 600 oysters (2.13 kg) were individually injected in the adductor muscle with 50 µL of viral suspension, containing 1.7×10^5 copies of OsHV-1 µVar μL^{-1} diluted by 10x (Schikorski *et al.* 2011). They were kept without feeding in a 45 L tank in static oxygenized seawater for 24 h where they shed viral particles (Fig. 1). At this point, the seawater surrounding the donors

became contaminated with the virus and used as the source of infection connected to the seawater distribution network by flexible tubes fitted inside a peristaltic pump (Pernet *et al.* 2021). Infection therefore began on day 14 of the experiment (Fig. 1B). The water input from the source of infection was arrested after 7 days of exposure. The donors were then removed. Survival of oysters placed in the virus-contaminated seawater (donors) and in the recipient tanks (level 3) was monitored daily for 16-20 d, and dead animals were removed at the end.

Due to logistical constraints, there was no uninfected control. In our experimental conditions, the survival of these controls is always 100%, so that they are generally excluded from the survival analyzes (see Pernet et al. 2021 and references therein). Therefore, we cannot decipher the effect of virus from that of time (and any potential confounding time-related effects) during the virus exposure phase.

Sampling

Oysters (N = 5 individuals) were sampled and weighted during acclimation at day 5, 12 and 14, and after virus exposure 72 h post-infection (hpi, 17 d) in each recipient tank (Fig. 1B). Soft tissues were removed from the shells, pooled together and flash frozen in liquid nitrogen and stored at −80°C. Samples were then ground in liquid nitrogen with a MM400 homogenizer and the resulting powder was subsampled for bacterial microbiota (metabarcoding), gene expression (RNA sequencing) and lipid (classes and fatty acid). Five oysters were also individually sampled in each tank 72 hpi and directly ground for OsHV-1 DNA detection. Tissues were immediately homogenized with a polytron homogenizer in 2 mL of sterile artificial seawater and stored at -20°C until analysis.

Seaweeds (2g) were sampled during acclimation at day 6, 11 and 14 d for metabarcoding analyses, and at day 14 for fatty acid analyses (Fig. 1B). As for oysters, seaweed samples were flash frozen in liquid nitrogen, stored at -80°C and ground in liquid nitrogen.

Seawater (*ca*. 1 mL) was sampled at 72 hpi at the inlet and outlet of the tanks containing the oysters for OsHV-1 DNA qPCR analyses (Fig. 1B). Seawater was stored in sterile 1.5 mL Eppendorf tubes at −20°C until analysis.

(c) Analyses

Quantification of OsHV-1

The detection and quantification of OsHV-1 DNA was carried out on seawater samples and individual oysters at 72 hpi, using a previously published qPCR protocol (Taqman, Martenot 2011) by Labocea, a French public diagnostic laboratory (Quimper, France, see File S1).

Bacterial microbiota analysis

Analyses were conducted as described in de Lorgeril et al (de Lorgeril *et al.* 2018). Briefly, DNA was extracted from 30 mg of frozen algae powders (sampled at days 6, 11 and 14) and oyster powders (sampled at days 5, 12, 14 and 17) using the DNA from tissue Macherey-Nagel kit (reference 740952.250). DNA concentration and purity were checked with the Nanodrop ND-1000 spectrometer. For each sample, 16S rDNA amplicon libraries were generated using the 341F-CCTACGGGNGGCWGCAG and 805R-GACTACHVGGGTATCTAATCC primers targeting the variable V3V4 loops for bacterial communities (Klindworth *et al.* 2013). Library were generated using the Illumina two-step PCR protocol and normalized SequalPrep plates. Paired-end sequencing with a 250-bp read length was performed at the Bio-Environnement UPVD technology platform (University of Perpignan Via Domitia Perpignan, France) on a MiSeq system (Illumina) using v2 chemistry according to the manufacturer's protocol. The FROGS

pipeline (Find Rapidly OTU with Galaxy Solution) implemented into a galaxy instance was used to define Operational Taxonomic Units (OTU) and to compute taxonomic affiliations (Escudié *et al.* 2018). Paired reads were merged using FLASH (Magoč & Salzberg 2011). After denoising and primer/adapter removal with Cutadapt (Martin 2011), clustering was performed with SWARM, which uses a clustering algorithm with a threshold (distance=3) corresponding to the maximum number of differences between two OTUs (Mahé *et al.* 2014). Chimeras were removed using VSEARCH (Rognes *et al.* 2016). We excluded chloroplasts from the dataset and filtered out singletons and produced affiliations using Blast against the Silva 16S rDNA database (release 132, Dec 2017) to produce an OTU and affiliation table in the standard BIOM format. Rarefaction curves of the species richness, confirming a sufficient sequencing, were generated using the Phyloseq R package and the rarefy_even_depth and ggrare functions (McMurdie & Holmes 2013). We used Phyloseq to obtain community composition and to infer diversity metrics at the OTU level using R v3.3.1 (R Development Core Team, R Foundation for Statistical Computing, Vienna, Austria [http://www.R- project.org]).

Transcriptome analyses

We analyzed the whole transcriptome of oysters to compare gene expression after 14 d of acclimation to different seaweeds. RNAs were extracted using 1.5 mL of Extract-All (EuroBio GEXEXT04 0U) from 30 mg of the oyster powders used for bacterial microbiota analysis (see sampling section). RNA concentration and purity were checked using the Nanodrop spectrometer, and their integrity was analyzed by capillary electrophoresis on a BioAnalyzer 2100 (Agilent). RNA-seq library construction and sequencing were performed at the Bio-Environment platform. PolyA+ libraries were constructed using the NEBNext Ultra II directionnal kit according to manufacturer's instructions from 1µg of total RNA and sequenced

on a NextSeq550 Instrument (SE 75 bp). Data were analyzed using a local galaxy instance (Goecks *et al.* 2010). Reads quality was checked using the Fastq-X toolkit and since all reads display a Phred score above 26 over 90% of their length, no subsequent quality filtering was done (Goecks *et al.* 2010). Adaptor trimming was then performed using CutAdapt (Martin 2011). Mapping to the *C. gigas* reference genome (assembly version V9 from (Zhang *et al.* 2012)) was performed using RNAstar using default parameters (Galaxy Version 2.4.0d-2 from (Dobin *et al.* 2012)). The HTSeq-count tool was used to count the number of reads overlapping annotated genes (Galaxy Version v0.6.1) (Anders *et al.* 2014). Differential gene expression levels were analyzed with the DESeq2 R package implemented into a galaxy instance (DESeq {DESeq2} from (Love *et al.* 2014)). Fold changes between conditions were considered significant when the adjusted p-value for multiple testing with the Benjamini-Hochberg procedure, which controls the false discovery rate (FDR), was < 0.05.

Gene ontology annotation analysis

Functional analyses of the differentially expressed genes (DEGs) were performed *de novo* on assembled transcripts using gene ontology annotation. Blastx comparison against the NR database was performed for the 28,027 genes annotated in the genome, with a maximum number of target hits of 20 and a minimum e-value of 0.001. XML blast result files were loaded onto Blast2GO (Conesa *et al.* 2005) for GO mapping and annotation with the b2g_sep13 version of the B2G database. GO terms of differentially expressed genes (DEGs, over- and under-expressed) and associated p-value (DESeq 2) were used as inputs for REVIGO (REduce + VIsualize Gene Ontology), to obtain hierarchical visualisation of non-redundant GO term set (Supek *et al.* 2011). Over-represented GO terms in one condition compared to another were

visualized using hierarchical treemaps (biological process) and scatterplots (molecular function).

Gross physiology of oysters

Although oysters are filter-feeders and do not directly fed on seaweed, they still might be exposed to dissolved and particulate compounds that potentially alter the response to pathogens. We therefore provide complementary measurements of host growth, food ingestion, energy reserves and trophic indicators to investigate potential confounders.

From daily measurements of phytoplankton concentration at the inlet and outlet of each oyster tank (see previous sections), we calculated the food consumption expressed in volume of microalgae consumed per minute once a day over the duration of the experiment. Daily ingestion rates were averaged over the acclimation periods for each condition and tank.

We evaluate the triacylglycerol to sterol ratio (TAG/ST) of oysters at the end of the acclimation period. The TAG/ST is indeed a proxy of physiological condition in marine organisms associated with disease resistance or tolerance in oysters (Pernet *et al.* 2019). A subsample of the oyster powder sampled at 14 d was placed in glass vials containing chloroform–methanol (2:1 v/v) and stored at −20°C under nitrogen until analyses (File S1).

We investigated with fatty acids whether the seaweed had contributed to the oyster diet. We analyzed the fatty acid composition of total lipids in seaweed (food sources) and of neutral lipids in oysters (consumers) as described in file S1. We consider that the fatty acid composition of a consumer reflects that of his food sources (“you are what you eat” principle), and that seaweed have very different fatty acid profiles depending on the species (Dalsgaard *et al.* 2003). Therefore, if the oysters have consumed seaweed, this will show in their fatty acid profile.

(d) Statistics

The survival time curves of oysters exposed to OsHV-1 were compared using the Cox regression model considering the effect of seaweed (4 levels, green, brown, red and control condition). Each tank was considered as cluster using the sandwich method to obtain robust parameter estimates. The proportionality of hazards (PH) was checked with martingale residuals.

Mixed-model ANOVAs were performed to assess differences in (1) prevalence and quantification of OsHV-1 DNA in oysters 72 hpi depending on seaweed (4 levels), (2) OsHV-1 DNA in seawater 72 hpi depending on seaweed (4 levels, main plot), levels (2 levels, inlet and outlet of the holding tank, subplots) and their interaction, and (3) oyster total body mass, ingestion rate, and physiological condition (triglyceride to sterol ratio) depending on seaweed (4 levels).

The unit of replication (random factor) was the tank in which the seaweed conditions were applied. Tukey's HSD was used as a post hoc test. The statistical threshold for rejection of the null hypothesis was set at 0.05. When $0.05<p<0.10$, power analysis was conducted to assess the probability of accepting the null hypothesis when it is false. In general, a power of 0.80 is acceptable. The normality of residuals and homogeneity of variances were graphically checked, and the data were log-transformed where necessary. Prevalence data were fitted a binomial distribution. When OsHV-1 DNA was detected but below the quantification threshold (10 cp ul^{-1}), individuals were considered positive and assigned the value of 10 cp mg^{-1} DNA. All these analyses were conducted with the SAS software package (SAS 9.4; SAS Institute, Cary, North Carolina, USA).

Microbial assemblages were compared across tissue types (algae and oysters) and sampling time according to the following procedure using R v3.3.1 (R Development Core Team, R Foundation for Statistical Computing, Vienna, Austria [http://www.R- project.org]). Principal coordinate analyses (PCoA, {phyloseq}) were computed to represent dissimilarities between samples using the Bray–Curtis distance matrix (ordinate, {phyloseq}). Multivariate homogeneity of group dispersions was tested between bacterial assemblages among samples using 999 permutations (permutest, betadisper, {vegan}). The 200 most abundant OTUs (to the lowest affiliated rank) were selected and used for DESeq2 analyses (DESeq {DESeq2}) to identify those whose abundance varied between conditions (Love *et al.* 2014). We first identified taxa whose relative abundance changed among conditions after the acclimation period by comparing oysters exposed for 14 days with a specific alga and their controls collected at the same time. Then, we identified taxa (genera) whose relative abundance changed during the infection phase by comparing oysters acclimated for 14 days with a specific alga and their counterparts exposed to the virus collected at 17 d. Heatmaps of taxa (genera) with significant changes in abundances during acclimation and infection phases were computed using the $\log_2$ of relative abundances and Multiple Array Viewer software (Supek *et al.* 2011).

3. Results

(a) Oyster survival and OsHV-1

Survival of oysters acclimated to green algae and further exposed to OsHV-1 was only 52 ± 5 %, compared to 66 ± 11 % for controls, 72 ± 17 % for brown algae, and 83 ± 13 % for red algae (Fig. 2A). Odds of oyster mortality was twice as high in the green algae condition as in the control (Table 1). Conversely, the probability of oyster mortality was half as high in the red algae conditions compared to the control. This result was close to statistical significance and

the power value of the test was low (0.523). There was no detectable difference in survival among oysters acclimated to brown algae and controls (Table 1).

The effect of seaweed on virus prevalence in oysters 72 hpi was close to statistical significance ($p<0.1$), but appeared higher in individuals acclimated to green algae (on all three tanks, 14 out of 15 individuals were positive) than in other conditions (<7 positive out of 15 individuals, Fig. 2B, Table S1). This trend was confirmed by higher amounts of viral DNA detected in oysters acclimated to green algae (Table 2). Virus load in seawater at the inlet of the oyster tanks were similar among conditions (between 9.8×10^3 and 1.7×10^4 OsHV-1 DNA copies mL^{-1}, Fig. S1).

(b) Bacterial microbiota

We analysed bacterial communities using 16S metabarcoding during acclimation in seaweeds and oysters (5-6, 11-12, 14 d) and infection in oysters (17 d). A total of 9,636,786 reads were obtained from 292 libraries. After the cleaning and filtering steps, 8,330,874 sequences were affiliated to 20,105 OTUs. After removing chloroplasts and non-bacteria, a total of 18,176 OTUs were kept for further analyses (Supplementary data 1, Fig. S2). The bacterial microbiota of algae varied among species and remained stable during the acclimation period (Figs 3A and S3, and PERMANOVAs Table S2). Diversity indices in algae did not change over time (Fig. S4).

The bacterial microbiota of oysters acclimated to green algae diverged from that of controls after 12 d while it remained similar for other conditions (Figs 3A and S3, PERMANOVA Tables S2 and S3). This was reflected in indices of bacterial diversity which all increased in oysters during acclimation to green algae while they remained stable for other conditions (Fig. S5).

During the virus exposure phase, the addition of OsHV-1 induced a shift in the bacterial microbiota of oysters held with brown algae and red algae and resulted in an increase in diversity indices (Fig. 3A and S5, PERMANOVA Tables S2 and S3). Overall, in the green algae condition, bacterial microbiota of oysters changed during the acclimation phase, whereas in

other conditions, changes occurred later during virus exposure. Class-level assignment of bacterial OTUs indicated that oysters acclimated to green algae showed a marked decrease in the relative abundance of *Mollicutes* at the benefit of *Alphaproteobacteria* between 5 d and 12 d (Fig. S3). These changes occurred in oysters held with brown or red algae later during virus exposure (17 d).

In addition, we analyzed bacterial communities (200 most abundant OTUs) at the genera level during acclimation to algae and virus exposure. The most significant changes occurred in oysters acclimated to green algae (compared to control at 14 d). The relative abundance of 28 OTUs changed (26 were over-represented, 4 of them belong to *Rhodobacteraceae*) and 20 of them were shared with algae (Fig. 3B). There was no difference in the relative abundance of OTUs between oysters acclimated to red algae and control (Fig. 3C). In oysters acclimated to brown algae, only 3 OTUs specific to oysters were modified (Fig. 3D).

Virus exposure was associated with significant changes in the relative abundance of OTUs in oysters acclimated to green algae (16 OTUs, 6 over-represented), brown algae (21 OTUs, 15 over-represented) and red algae (22 OTUs, 12 over-represented) (Fig. 3B-D). Among these OTUs, 7 were common to the three conditions. Four genera were over-represented (*Aureispira*, *Poseidonocella*, *Roseovarius* and *Olleya*), the others were under-represented (*Salinirepens*, *Flavobacteriaceae* and *Ulvibacter*). Two of these over-represented OTUs were detected in green algae at the beginning of the acclimation phase (genera *Poseidonocella* and *Olleya*, Fig. 3B-D). It is noteworthy that the relative abundance of one OTU corresponding to the genus *Vibrio* increased during infection in oysters acclimated to green algae.

(c) Oyster transcriptomic response

We compared the transcriptomic response of oysters acclimated to green, brown and red algae with that of controls. We sequenced 12 samples that yielded between 25 and 30 millions

Illumina single-end reads of 75 bp per sample. Between 96.4% and 96.9% of these reads mapped to the *C. gigas* V9 reference genome and were used for identification of differential expressed genes (DEGs). The transcriptome of oysters in contact with algae was modified compared to untreated controls (Fig. 4A). We found 311 DEGs (222 over-expressed) in oysters acclimated to green algae vs. control oysters, compared to 299 and 128 DEGs in those held with brown and red algae respectively (167 and 55 over-expressed respectively, Fig. 4A and Supplementary data 2). DEGs were predominantly specific to each seaweed, very few DEGs were shared among all conditions.

Functional analyses of DEGs by condition showed that the defense response was the only category of biological process that was enriched in the three conditions. Defense response category was the second over-represented category in oysters acclimated to green algae, the first over-represented category in oysters acclimated to red algae and was found under “RNA secondary structure unwinding” category in oysters acclimated to brown algae (Fig. S6). As observed for all DEGs, the number of DEGs related to defense response was the highest in oysters acclimated to green algae (32, 22 up-regulated), intermediate in oysters held with brown algae (26, 13 up-regulated) and the lowest in oysters acclimated to red algae (9, 2 up-regulated) (Fig. 4B). No common DEG for this category was identified between the three conditions. In oyster acclimated to green algae, the DEGs related to defense response were mainly associated to potential immune recognition proteins like complement C1q, C- and P-lectin (Perlucin and cation-dependent mannose-6-phosphate receptor), tolloid-like, scavenger receptor (Deleted in malignant brain tumors 1 –like) and low affinity immunoglobulin epsilon Fc receptor and to enzymes like laccase and tyrosinase (Fig. 4C, Supplementary data 2). In addition, DEGs related to defense response were mainly associated, in term of molecular

function, to binding function to carbohydrate, calcium ion, metal ion, zinc ion, protein, copper ion, TIR domain, RNA and DNA (Fig. S7).

(d) Gross physiology

We measured host growth, food ingestion, energy reserves and trophic indicators, to investigate potential confounders. None of these parameters were affected by seaweed (Fig. S8). At the onset of the virus exposure, total body mass and energy reserves (lipid, TAG/ST) and food ingestion were similar among conditions. Also, fatty acid compositions of green, brown and red algae were different and did not reflect in the neutral lipid of oysters, suggesting that seaweeds did not contribute to their food regime.

4. Discussion

Here we showed that different species of seaweeds can positively or negatively influence the risk of disease in oysters by shaping their bacterial microbiota and their immune response. Although seaweed and oysters do not have direct ecological interactions, they are connected by seawater and share microbes. Our study therefore extends the concept of pathobiome beyond recognized pathogens to other ecosystem components, and contributes to establishing a community perspective of host-pathogen interactions (Dittami *et al.* 2021). These results are therefore important to better understand the risk of disease in marine ecosystems. The study framework developed here can be applied to other analogous systems of interaction than the specific one of algae and oysters, such as those particularly threatened by diseases including corals, amphibians and farmed organisms.

We found that green algae belonging to the genus *Ulva* spp. increased mortality and virus proliferation in the host, induced early dysbiosis of the host's bacterial microbiota and overexpression of genes involved in defense response. Although field studies showed that the

proliferation of green algae has dramatic impacts on macro-zoobenthic and microbial communities (Quillien *et al.* 2015; Wang *et al.* 2020), no studies to date have established a link with the POMS or other marine diseases. Our results suggest that the rising tide of green algal bloom worldwide due to human-induced eutrophication (Ye *et al.* 2011; Smetacek & Zingone 2013) may have consequences on oyster-pathogen interactions and disease risk. More broadly, our results are in agreement with the fact that environmental and human-mediated disturbances of natural ecosystems can shape bacterial pathobiomes and promote the emergence of diseases (Vayssier-Taussat *et al.* 2014). For instance, invasive exotic annual grasses can indirectly increase barley and cereal yellow dwarf virus disease incidence in California native perennial bunchgrasses (Malmstrom *et al.* 2005).

Our results on oysters differ from those obtained on the shrimp *Litopenaeus vannamei*. Indeed, the green algae *Ulva lactuca* positively influence their microbiota (Mangott *et al.* 2020) and improve their resistance to bacterial and viral diseases though immune and anti-oxidant responses (Anaya-Rosas *et al.* 2019). This discrepancy, which possibly reflect specific differences between host organisms and their immune defense mechanisms, underscores the importance of developing this study framework on other species.

Dysbiosis in oysters acclimated to green algae *Ulva* spp*.* consisted of an increase in bacterial diversity, a decrease relative abundance of bacteria from the class *Mollicutes* at the benefit of *Alphaproteobacteria*, and overrepresentation of the family *Rhodobacteraceae*. Although bacterial diversity is often associated with better health of the host community, this is not always the case (Bass *et al.* 2019). Tissue damage from infections can promote colonization by a wide variety of opportunistic bacteria from the surrounding environment. This is what happens during OsHV-1 infection (see de Lorgeril *et al.* 2018; Lucasson *et al.* 2020 and this

study), and in other diseases affecting corals (Closek *et al.* 2014; Roder *et al.* 2014). The shift in the relative abundance of *Mollicutes* at the benefit of *Alphaproteobacteria* has never been reported before. In contrast, *Mollicutes* can be more abundant in diseased oysters than in healthy ones but not always (King *et al.* 2019; Clerissi *et al.* 2020). This agrees with the 'Anna Karenina principle' for animal microbiomes, in which dysbiotic individuals vary more in microbial community composition than healthy individuals (Zaneveld *et al.* 2017). Finally, the potential role of bacteria from the *Rhodobacteraceae* family remains unclear. These bacteria were associated with juvenile oyster disease (Boettcher *et al.* 2005) but also with resistance to POMS (Clerissi *et al.* 2020).

During infection, the relative abundance of 4 OTUs belonging to the genera *Poseidonocella, Aureispira, Roseovarius* and *Olleya* increased under all conditions, suggesting that these bacterial genera are involved in the secondary phase of POMS, i.e. colonization by opportunistic bacterial pathogens leading to the death of oysters (de Lorgeril *et al.* 2018). *Poseidonocella* and *Olleya* were overrepresented in *Ulva* spp. and in the oysters during acclimation and may have increased susceptibility to POMS. During infection we observed in oysters acclimated to green algae an increase of the relative abundance of *Vibrio*, a genus of bacteria previously associated to POMS (Petton *et al.* 2015b; de Lorgeril *et al.* 2018; King *et al.* 2019; Clerissi *et al.* 2020). However, we did not observe this increase in oysters held with red (*Solieria chordalis*) and brown algae (*Fucus vesiculosus*).

Although dysbiosis clearly appeared in oysters acclimated to *Ulva* spp., a causal relationship with viral proliferation in the host and increased mortality was not established. However, transcriptomic analysis revealed that oysters acclimated to these green algae overexpressed genes primarily related to the defense mechanism. Among these genes, we found laccase and

tyrosinase, two enzymes of the phenoloxidase system involved in immune, antioxidant and detoxification responses in bivalves that potentially have a protective role against bacterial infection (Luna-Acosta *et al.* 2017; Quinn *et al.* 2020). Therefore, transcriptomic analysis supports dysbiosis as a major consequence for oysters held with green algae.

More broadly, the transcriptomic analysis reveals that the number of differentially expressed genes (DEGs), including those related to the defense response, was highest in oysters acclimated to green algae *Ulva* spp., intermediate in oysters maintained with brown algae *F. vesiculosus* and lowest in oysters acclimated to red algae *S. chordalis*. Therefore, the number of DEGs seems to be associated with the risk of disease-induced mortality according to the different types of algae and is a good indicator of stress.

We further observe that red algae have a positive but weak effect on oyster survival. Considering that the statistical power is low, the experiment should be repeated with a higher number of replications.

In conclusion, the present work show that algae can alter the bacterial microbiota, immune status and disease outcome of oysters, thus highlighting the importance of considering macro and microbiotic interactions in disease, ecosystem and farm management. These considerations are particularly applicable to the development of integrated multi-trophic aquaculture, co-culture, or any other practice that relies on increasing biological diversity to increase resilience of marine ecosystems to global change (see for example Groner *et al.* 2018; Falkenberg *et al.* 2021). We however suggest that future research should evaluate these interactions in natural field condition where oysters, OsHV-1 and seaweeds coexist.

Data accessibility

Amplicon sequences for microbiota analysis and RNA-seq data have been made available through the SRA database (BioProject accession number PRJNA731543 with SRA accession SRP322069). Other data are submitted as electronic supplementary material and deposited at the SEANOE Digital Repository https://doi.org/10.17882/85142.

Authors' contributions

E.D, B.P. and F.P. designed the study and conducted the experiment, and E.D, J.D.L., E.T. and Y.G. performed bacterial microbiota and transcriptome analyses, E.D., J.D.L., E.T., Y.G. and F.P. analyzed the data. E.D. and F.P. wrote the manuscript together. All authors contributed and approved the paper.

Competing interests

We declare we have no competing interests.

Funding

This work was funded by the EU funded projects VIVALDI (H2020 program, n°678589) and FEDIVER (DLAL/FEAMP).

Acknowledgments

We thank the Ifremer staff involved in oyster and algae production at Ifremer Argenton and Bouin. We are grateful to M. Hubert for helping with the experimental set-up, to B. Morga and N. Faury for providing viral suspension, to V. Le Roy and C. Quéré for lipid analyses, to C. Dubreuil for RNA and DNA extraction and J.-F. Allienne for supporting library construction and sequencing. We are grateful to V. Stiger-Pouvreau and E. Deslandes for their expertise with seaweeds.

References

Anaya-Rosas, R.E., Rivas-Vega, M.E., Miranda-Baeza, A., Piña-Valdez, P. & Nieves-Soto, M. (2019) Effects of a co-culture of marine algae and shrimp (*Litopenaeus vannamei*) on

the growth, survival and immune response of shrimp infected with *Vibrio parahaemolyticus* and white spot virus (WSSV). *Fish & Shellfish Immunology,* **87,** 136-143. https://dx.doi.org/10.1016/j.fsi.2018.12.071

Anders, S., Pyl, P.T. & Huber, W. (2014) HTSeq—a Python framework to work with high-throughput sequencing data. *Bioinformatics,* **31,** 166-169. https://dx.doi.org/10.1093/bioinformatics/btu638

Bass, D., Stentiford, G.D., Wang, H.-C., Koskella, B. & Tyler, C.R. (2019) The Pathobiome in Animal and Plant Diseases. *Trends in Ecology & Evolution,* **34,** 996-1008. https://dx.doi.org/10.1016/j.tree.2019.07.012

Ben-Horin, T., Bidegain, G., Huey, L., Narvaez, D.A. & Bushek, D. (2015) Parasite transmission through particle feeding. *Journal of Invertebrate Pathology,* **131,** 155–176. https://dx.doi.org/10.1016/j.jip.2015.07.006

Boettcher, K.J., Geaghan, K.K., Maloy, A.P. & Barber, B.J. (2005) *Roseovarius crassostreae* sp. nov., a member of the Roseobacter clade and the apparent cause of juvenile oyster disease (JOD) in cultured Eastern oysters. *International Journal of Systematic and Evolutionary Microbiology,* **55,** 1531-1537. https://dx.doi.org/10.1099/ijs.0.63620-0

Byers, J.E. (2020) Effects of climate change on parasites and disease in estuarine and nearshore environments. *PLoS biology,* **18,** e3000743. https://dx.doi.org/10.1371/journal.pbio.3000743

Clerissi, C., de Lorgeril, J., Petton, B., Lucasson, A., Escoubas, J.-M., Gueguen, Y., Dégremont, L., Mitta, G. & Toulza, E. (2020) Microbiota Composition and Evenness Predict Survival Rate of Oysters Confronted to Pacific Oyster Mortality Syndrome. *Frontiers in microbiology,* **11,** 311-311. https://dx.doi.org/10.3389/fmicb.2020.00311

Closek, C.J., Sunagawa, S., DeSalvo, M.K., Piceno, Y.M., DeSantis, T.Z., Brodie, E.L., Weber, M.X., Voolstra, C.R., Andersen, G.L. & Medina, M. (2014) Coral transcriptome and bacterial community profiles reveal distinct Yellow Band Disease states in *Orbicella faveolata*. *The Isme Journal,* **8,** 2411-2422. https://dx.doi.org/10.1038/ismej.2014.85

Conesa, A., Götz, S., García-Gómez, J.M., Terol, J., Talón, M. & Robles, M. (2005) Blast2GO: a universal tool for annotation, visualization and analysis in functional genomics research. *Bioinformatics,* **21,** 3674-3676. https://dx.doi.org/10.1093/bioinformatics/bti610

Cory, J.S. & Deschodt, P.S. (2017) The Biotic Environment. *Ecology of Invertebrate Diseases*, pp. 187-212. https://dx.doi.org/10.1002/9781119256106.ch6

Dalsgaard, J., St. John, M., Kattner, G., Muller-Navarra, D. & Hagen, W. (2003) Fatty acid trophic markers in the pelagic marine environment. *Advances in Marine Biology,* **46,** 225-340. https://dx.doi.org/10.1016/S0065-2881(03)46005-7

de Lorgeril, J., Lucasson, A., Petton, B., Toulza, E., Montagnani, C., Clerissi, C., Vidal-Dupiol, J., Chaparro, C., Galinier, R., Escoubas, J.-M., Haffner, P., Dégremont, L., Charrière, G.M., Lafont, M., Delort, A., Vergnes, A., Chiarello, M., Faury, N., Rubio, T., Leroy, M.A., Pérignon, A., Régler, D., Morga, B., Alunno-Bruscia, M., Boudry, P., Le Roux, F., Destoumieux-Garzón, D., Gueguen, Y. & Mitta, G. (2018) Immune-suppression by OsHV-1 viral infection causes fatal bacteraemia in Pacific oysters. *Nature Communications,* **9,** 4215. https://dx.doi.org/10.1038/s41467-018-06659-3

Dittami, S.M., Arboleda, E., Auguet, J.-C., Bigalke, A., Briand, E., Cárdenas, P., Cardini, U., Decelle, J., Engelen, A.H., Eveillard, D., Gachon, C.M.M., Griffiths, S.M., Harder, T., Kayal, E., Kazamia, E., Lallier, F.H., Medina, M., Marzinelli, E.M., Morganti, T.M., Núñez Pons, L., Prado, S., Pintado, J., Saha, M., Selosse, M.-A., Skillings, D., Stock, W.,

Sunagawa, S., Toulza, E., Vorobev, A., Leblanc, C. & Not, F. (2021) A community perspective on the concept of marine holobionts: current status, challenges, and future directions. *Peerj,* **9,** e10911. https://dx.doi.org/10.7717/peerj.10911

Dobin, A., Davis, C.A., Schlesinger, F., Drenkow, J., Zaleski, C., Jha, S., Batut, P., Chaisson, M. & Gingeras, T.R. (2012) STAR: ultrafast universal RNA-seq aligner. *Bioinformatics,* **29,** 15-21. https://dx.doi.org/10.1093/bioinformatics/bts635

Dupont, S., Lokmer, A., Corre, E., Auguet, J.C., Petton, B., Toulza, E., Montagnani, C., Tanguy, G., Pecqueur, D., Salmeron, C., Guillou, L., Desnues, C., La Scola, B., Bou Khalil, J., de Lorgeril, J., Mitta, G., Gueguen, Y. & Escoubas, J.M. (2020) Oyster hemolymph is a complex and dynamic ecosystem hosting bacteria, protists and viruses. *Animal Microbiome,* **2,** 12. https://dx.doi.org/10.1186/s42523-020-00032-w

Egan, S., Harder, T., Burke, C., Steinberg, P., Kjelleberg, S. & Thomas, T. (2013) The seaweed holobiont: understanding seaweed–bacteria interactions. *FEMS Microbiology Reviews,* **37,** 462-476. https://dx.doi.org/10.1111/1574-6976.12011

Escudié, F., Auer, L., Bernard, M., Mariadassou, M., Cauquil, L., Vidal, K., Maman, S., Hernandez-Raquet, G., Combes, S. & Pascal, G. (2018) FROGS: Find, Rapidly, OTUs with Galaxy Solution. *Bioinformatics,* **34,** 1287-1294. https://dx.doi.org/10.1093/bioinformatics/btx791

Falkenberg, L.J., Scanes, E., Ducker, J. & Ross, P.M. (2021) Biotic habitats as refugia under ocean acidification. *Conservation Physiology,* **9,** coab077. https://dx.doi.org/10.1093/conphys/coab077

Floc'h, J.Y., Deslandes, E. & Gall, Y.L. (1987) Evidence for Vegetative Propagation of the Carrageenophyte *Solieria chordalis* (Solieriaceae, Rhodophyceae) on the Coast of

Brittany (France) and in Culture. *Botanica Marina,* **30,** 315-322. https://dx.doi.org/10.1515/botm.1987.30.4.315

Goecks, J., Nekrutenko, A., Taylor, J. & The Galaxy, T. (2010) Galaxy: a comprehensive approach for supporting accessible, reproducible, and transparent computational research in the life sciences. *Genome Biology,* **11,** R86. https://dx.doi.org/10.1186/gb-2010-11-8-r86

Groner, M.L., Burge, C.A., Cox, R., Rivlin, N.D., Turner, M., Van Alstyne, K.L., Wyllie-Echeverria, S., Bucci, J., Staudigel, P. & Friedman, C.S. (2018) Oysters and eelgrass: potential partners in a high pCO(2) ocean. *Ecology,* **99,** 1802-1814. https://dx.doi.org/10.1002/ecy.2393

Hily, C. & Jean, F. (1997) Macrobenthic biodiversity in intertidal habitats of the Iroise Biosphere Reserve (Brittany, France). *Journal of the Marine Biological Association of the United Kingdom,* **77,** 311-323. https://dx.doi.org/10.1017/S0025315400071691

King, W.L., Jenkins, C., Go, J., Siboni, N., Seymour, J.R. & Labbate, M. (2019) Characterisation of the Pacific oyster microbiome during a summer mortality event. *Microbial Ecology,* **77,** 502-512. https://dx.doi.org/10.1007/s00248-018-1226-9

Klindworth, A., Pruesse, E., Schweer, T., Peplies, J., Quast, C., Horn, M. & Glöckner, F.O. (2013) Evaluation of general 16S ribosomal RNA gene PCR primers for classical and next-generation sequencing-based diversity studies. *Nucleic Acids Research,* **41,** e1. https://dx.doi.org/10.1093/nar/gks808

Lachnit, T., Meske, D., Wahl, M., Harder, T. & Schmitz, R. (2011) Epibacterial community patterns on marine macroalgae are host-specific but temporally variable. *Environmental Microbiology,* **13,** 655-665. https://dx.doi.org/10.1111/j.1462-2920.2010.02371.x

Le Roux, F., Wegner, K.M. & Polz, M.F. (2016) Oysters and Vibrios as a Model for Disease Dynamics in Wild Animals. *Trends in Microbiology,* **24,** 568-580. https://dx.doi.org/10.1016/j.tim.2016.03.006

Lokmer, A., Kuenzel, S., Baines, J.F. & Wegner, K.M. (2016) The role of tissue-specific microbiota in initial establishment success of Pacific oysters. *Environmental Microbiology,* **18,** 970-987. https://dx.doi.org/10.1111/1462-2920.13163

Lokmer, A. & Wegner, M.K. (2015) Hemolymph microbiome of Pacific oysters in response to temperature, temperature stress and infection. *The Isme Journal,* **9,** 670-682. https://dx.doi.org/10.1038/ismej.2014.160

Love, M.I., Huber, W. & Anders, S. (2014) Moderated estimation of fold change and dispersion for RNA-seq data with DESeq2. *Genome Biology,* **15,** 550. https://dx.doi.org/10.1186/s13059-014-0550-8

Lucasson, A., Luo, X., Mortaza, S., de Lorgeril, J., Toulza, E., Petton, B., Escoubas, J.-M., Clerissi, C., Dégremont, L., Gueguen, Y., Destoumieux-Garzón, D., Jacq, A. & Mitta, G. (2020) A core of functionally complementary bacteria colonizes oysters in Pacific Oyster Mortality Syndrome. *bioRxiv***,** 2020.2011.2016.384644. https://dx.doi.org/10.1101/2020.11.16.384644

Luna-Acosta, A., Breitwieser, M., Renault, T. & Thomas-Guyon, H. (2017) Recent findings on phenoloxidases in bivalves. *Marine Pollution Bulletin,* **122,** 5-16. https://dx.doi.org/10.1016/j.marpolbul.2017.06.031

Magoč, T. & Salzberg, S.L. (2011) FLASH: fast length adjustment of short reads to improve genome assemblies. *Bioinformatics,* **27,** 2957-2963. https://dx.doi.org/10.1093/bioinformatics/btr507

Mahé, F., Rognes, T., Quince, C., de Vargas, C. & Dunthorn, M. (2014) Swarm: robust and fast clustering method for amplicon-based studies. *Peerj,* **2,** e593. https://dx.doi.org/10.7717/peerj.593

Malmstrom, C.M., McCullough, A.J., Johnson, H.A., Newton, L.A. & Borer, E.T. (2005) Invasive annual grasses indirectly increase virus incidence in California native perennial bunchgrasses. *Oecologia,* **145,** 153-164. https://dx.doi.org/10.1007/s00442-005-0099-z

Mangott, A., Nappi, J., Delli Paoli Carini, A., Goncalves, P., Hua, K., Domingos, J.A., de Nys, R. & Thomas, T. (2020) *Ulva lactuca* as a functional ingredient and water bioremediator positively influences the hepatopancreas and water microbiota in the rearing of *Litopenaeus vannamei*. *Algal Research,* **51,** 102040. https://dx.doi.org/10.1016/j.algal.2020.102040

Martin, M. (2011) Cutadapt removes adapter sequences from high-throughput sequencing reads. *EMBnet journal,* **17,** 3. https://dx.doi.org/10.14806/ej.17.1.200

McMurdie, P.J. & Holmes, S. (2013) phyloseq: An R Package for Reproducible Interactive Analysis and Graphics of Microbiome Census Data. *PLoS ONE,* **8,** e61217. https://dx.doi.org/10.1371/journal.pone.0061217

Morand, P. & Merceron, M. (2005) Macroalgal Population and Sustainability. *Journal of Coastal Research,* **2005,** 1009-1020, 1012. https://dx.doi.org/10.2112/04-700A.1

Pathirana, E., Fuhrmann, M., Whittington, R. & Hick, P. (2019) Influence of environment on the pathogenesis of Ostreid herpesvirus-1 (OsHV-1) infections in Pacific oysters (*Crassostrea gigas*) through differential microbiome responses. *Heliyon,* **5,** e02101. https://dx.doi.org/10.1016/j.heliyon.2019.e02101

Pernet, F., Lagarde, F., Gall, P.L. & D'orbcastel, E.R. (2014) Associations between farming practices and disease mortality of oysters *Crassostrea gigas* in a Mediterranean

lagoon. *Aquaculture Environment Interactions,* **5,** 99-106. https://dx.doi.org/10.3354/aei00096

Pernet, F., Lugué, K. & Petton, B. (2021) Competition for food reduces disease susceptibility in a marine invertebrate. *Ecosphere,* **12**. https://dx.doi.org/10.1002/ecs2.3435

Pernet, F., Lupo, C., Bacher, C. & Whittington, R.J. (2016) Infectious diseases in oyster aquaculture require a new integrated approach. *Philosophical Transactions of the Royal Society of London. Series B: Biological Sciences,* **371,** 20150213. https://dx.doi.org/10.1098/rstb.2015.0213

Pernet, F., Tamayo, D., Fuhrmann, M. & Petton, B. (2019) Deciphering the effect of food availability, growth and host condition on disease susceptibility in a marine invertebrate. *The Journal of Experimental Biology,* **222**. https://dx.doi.org/10.1242/jeb.210534

Petton, B., Boudry, P., Alunno-Bruscia, M. & Pernet, F. (2015a) Factors influencing disease-induced mortality of Pacific oysters *Crassostrea gigas*. *Aquaculture Environment Interactions,* **6,** 205-222. https://dx.doi.org/10.3354/aei00125

Petton, B., Bruto, M., James, A., Labreuche, Y., Alunno Bruscia, M. & Le Roux, F. (2015b) *Crassostrea gigas* mortality in France: the usual suspect, a herpes virus, may not be the killer in this polymicrobial opportunistic disease. *Frontiers in microbiology,* **6,** 686. https://dx.doi.org/10.3389/fmicb.2015.00686

Quillien, N., Nordström, M.C., Guyonnet, B., Maguer, M., Le Garrec, V., Bonsdorff, E. & Grall, J. (2015) Large-scale effects of green tides on macrotidal sandy beaches: Habitat-specific responses of zoobenthos. *Estuarine Coastal and Shelf Science,* **164,** 379-391. https://dx.doi.org/10.1016/j.ecss.2015.07.042

Quinn, E.A., Malkin, S.H., Rowley, A.F. & Coates, C.J. (2020) Laccase and catecholoxidase activities contribute to innate immunity in slipper limpets, *Crepidula fornicata*. *Developmental and Comparative Immunology,* **110,** 103724. https://dx.doi.org/10.1016/j.dci.2020.103724

Roder, C., Arif, C., Bayer, T., Aranda, M., Daniels, C., Shibl, A., Chavanich, S. & Voolstra, C.R. (2014) Bacterial profiling of White Plague Disease in a comparative coral species framework. *The Isme Journal,* **8,** 31-39. https://dx.doi.org/10.1038/ismej.2013.127

Rognes, T., Flouri, T., Nichols, B., Quince, C. & Mahé, F. (2016) VSEARCH: a versatile open source tool for metagenomics. *Peerj,* **4,** e2584. https://dx.doi.org/10.7717/peerj.2584

Schikorski, D., Faury, N., Pepin, J.F., Saulnier, D., Tourbiez, D. & Renault, T. (2011) Experimental ostreid herpesvirus 1 infection of the Pacific oyster *Crassostrea gigas*: Kinetics of virus DNA detection by q-PCR in seawater and in oyster samples. *Virus Research,* **155,** 28-34. https://dx.doi.org/10.1016/j.virusres.2010.07.031

Singh, R.P. & Reddy, C.R.K. (2014) Seaweed–microbial interactions: key functions of seaweed-associated bacteria. *Fems Microbiology Ecology,* **88,** 213-230. https://dx.doi.org/10.1111/1574-6941.12297

Smetacek, V. & Zingone, A. (2013) Green and golden seaweed tides on the rise. *Nature,* **504,** 84. https://dx.doi.org/10.1038/nature12860

Supek, F., Bošnjak, M., Škunca, N. & Šmuc, T. (2011) REVIGO Summarizes and Visualizes Long Lists of Gene Ontology Terms. *PLoS ONE,* **6,** e21800. https://dx.doi.org/10.1371/journal.pone.0021800

Suquet, M., de Kermoysan, G., Araya, R.G., Queau, I., Lebrun, L., Le Souchu, P. & Mingant, C. (2009) Anesthesia in Pacific oyster, *Crassostrea gigas*. *Aquatic Living Resources,* **22,** 29-34. https://dx.doi.org/10.1051/alr/2009006

Sweet, M.J. & Bulling, M.T. (2017) On the Importance of the Microbiome and Pathobiome in Coral Health and Disease. *Frontiers in Marine Science,* **4**. https://dx.doi.org/10.3389/fmars.2017.00009

Vayssier-Taussat, M., Albina, E., Citti, C., Cosson, J.F., Jacques, M.-A., LEBRUN, M.-H., Le Loir, Y., Ogliastro, M., Petit, M.-A., Roumagnac, P. & Candresse, T. (2014) Shifting the paradigm from pathogens to pathobiome: new concepts in the light of meta-omics. *Frontiers in Cellular and Infection Microbiology,* **4,** 29. https://dx.doi.org/10.3389/fcimb.2014.00029

Wang, J., Lu, J., Zhang, Y. & Wu, J. (2020) Microbial ecology might serve as new indicator for the influence of green tide on the coastal water quality: Assessment the bioturbation of Ulva prolifera outbreak on bacterial community in coastal waters. *Ecological Indicators,* **113,** 106211. https://dx.doi.org/10.1016/j.ecolind.2020.106211

Wegner, K.M., Volkenborn, N., Peter, H. & Eiler, A. (2013) Disturbance induced decoupling between host genetics and composition of the associated microbiome. *BMC Microbiology,* **13,** 252. https://dx.doi.org/10.1186/1471-2180-13-252

Ye, N.-h., Zhang, X.-w., Mao, Y.-z., Liang, C.-w., Xu, D., Zou, J., Zhuang, Z.-m. & Wang, Q.-y. (2011) 'Green tides' are overwhelming the coastline of our blue planet: taking the world's largest example. *Ecological Research,* **26,** 477. https://dx.doi.org/10.1007/s11284-011-0821-8

Zaneveld, J.R., McMinds, R. & Vega Thurber, R. (2017) Stress and stability: applying the Anna Karenina principle to animal microbiomes. *Nature Microbiology,* **2,** 17121. https://dx.doi.org/10.1038/nmicrobiol.2017.121

Zhang, G., Fang, X., Guo, X., Li, L., Luo, R., Xu, F., Yang, P., Zhang, L., Wang, X., Qi, H., Xiong, Z., Que, H., Xie, Y., Holland, P.W.H., Paps, J., Zhu, Y., Wu, F., Chen, Y., Wang, J., Peng, C.,

Meng, J., Yang, L., Liu, J., Wen, B., Zhang, N., Huang, Z., Zhu, Q., Feng, Y., Mount, A., Hedgecock, D., Xu, Z., Liu, Y., Domazet-Lošo, T., Du, Y., Sun, X., Zhang, S., Liu, B., Cheng, P., Jiang, X., Li, J., Fan, D., Wang, W., Fu, W., Wang, T., Wang, B., Zhang, J., Peng, Z., Li, Y., Li, N., Wang, J., Chen, M., He, Y., Tan, F., Song, X., Zheng, Q., Huang, R., Yang, H., Du, X., Chen, L., Yang, M., Gaffney, P.M., Wang, S., Luo, L., She, Z., Ming, Y., Huang, W., Zhang, S., Huang, B., Zhang, Y., Qu, T., Ni, P., Miao, G., Wang, J., Wang, Q., Steinberg, C.E.W., Wang, H., Li, N., Qian, L., Zhang, G., Li, Y., Yang, H., Liu, X., Wang, J., Yin, Y. & Wang, J. (2012) The oyster genome reveals stress adaptation and complexity of shell formation. *Nature,* **490,** 49-54. https://dx.doi.org/10.1038/nature11413

Table 1. Cox regression model for survival data of oysters acclimated to seaweed and exposed to OsHV-1. Control oysters with no algae were used as reference.

Condition	df	Estimate	SE	χ^2	*P*	Odds ratio
Brown	1	-0.203	0.360	0.318	0.573	0.816
Green	1	0.662	0.190	12.175	0.001	1.939
Red	1	-0.776	0.432	3.227	0.072	0.460

Table 2. Levels of OsHV-1 DNA (cp mg^{-1}) in oysters acclimated to seaweed and exposed to the virus 72 hpi. Data are means ± SD (n=3 tanks). Summary of ANOVA performed on log-transformed data. Means sharing a letter are not statistically different (Tukey-adjusted comparisons). Abbreviations: SE, standard error; ddf, denominator degree of freedom.

Condition	OsHV-1 DNA	ANOVA (*F*=4.85, P=0.033)				
		Estimate	SE	ddf	*t* value	P
Green	$3.3\ 10^5 \pm 5.2\ 10^5$	2.053[a]	0.349	8	5.88	0.000
Brown	$7.7\ 10^1 \pm 1.3\ 10^2$	0.578[b]	0.349	8	1.66	0.136
Red	$4.6\ 10^4 \pm 8.0\ 10^4$	0.906[b]	0.349	8	2.60	0.032
Control	$2.7\ 10^2 \pm 4.6\ 10^2$	0.307[b]	0.349	8	0.88	0.405

Fig. captions

Fig. 1. Experimental design (A) and sampling schedule (B). Only one replicate out of three is represented. Arrows indicate direction of water flow. Each experimental unit consists of a header tank containing seaweed (or control) flowing to a holding tank containing oysters.

Fig. 2. Survival of oysters exposed to OsHV-1 after acclimation with seaweed (A) and prevalence of OsHV-1 in oysters (B). The thin lines in graph A represent the survival curves for each individual tank while the thick line is the average by condition. The y axis of graph B is the number of oysters positive to OsHV-1 out of 5 tested for each tank and condition 72 hpi. There are three bars per condition, each corresponding to one tank (replicate). The dark part of the bars represents positive individuals while the light part represents individuals for whom the virus was not detected (negative). Star indicates statistically significant differences.

Fig. 3. Bacterial microbiota in oysters during acclimation to seaweed and virus exposure. Multidimensional Scaling (MDS) plot of the Bray-Curtis dissimilarity matrix of the microbiota (A). Each point of the triangles corresponds to one of the 3 replicates at one time. Dots represent distinct pools of 5 oysters. Colors correspond to algal species and numbers refer to days. Heatmaps of the bacterial taxa that were modified in oysters during acclimation to algae and virus exposure (B-D). Significant changes in taxa were evaluated by DEseq during acclimation (seaweed vs control at 14 d) and virus exposure (17 d vs 14 d within algae). The numbers in red indicate taxa whose relative abundance was modified in all conditions during virus exposure. OTUs are classified according the value of DEseq fold change (higher to lower) and clustered in four groups. Groups I and II include taxa whose relative abundances increased or decreased respectively during acclimation to algae whereas group III and IV include those that increased or decreased, respectively, during virus exposure. Analyses were performed at

the genera level. The algae column corresponds to relative abundance of the bacterial taxa in algae at the beginning of the experiment (0 d) that were modified in oysters. The intensity level of the blue represents the relative abundance of bacterial taxa. At each time, the analysis was performed on 3 distinct pools of 5 oysters or 3 algae samples.

Fig. 4. Transcriptomic response of oysters. Venn diagrams of all DEGs (A) and DEGs related to defense (B) relatives to control oysters. (C) Heatmaps of the enriched GO categories for DEGs related to defenses (log2 Foldchange, p-adj < 0.05). The intensity of the enrichment is expressed as the ratio between the number of genes that were up (yellow heat) or down (blue heat) regulated compared with the total number of genes in the category. If the intensity was equal to zero (black heat), then the enrichment was not significant.

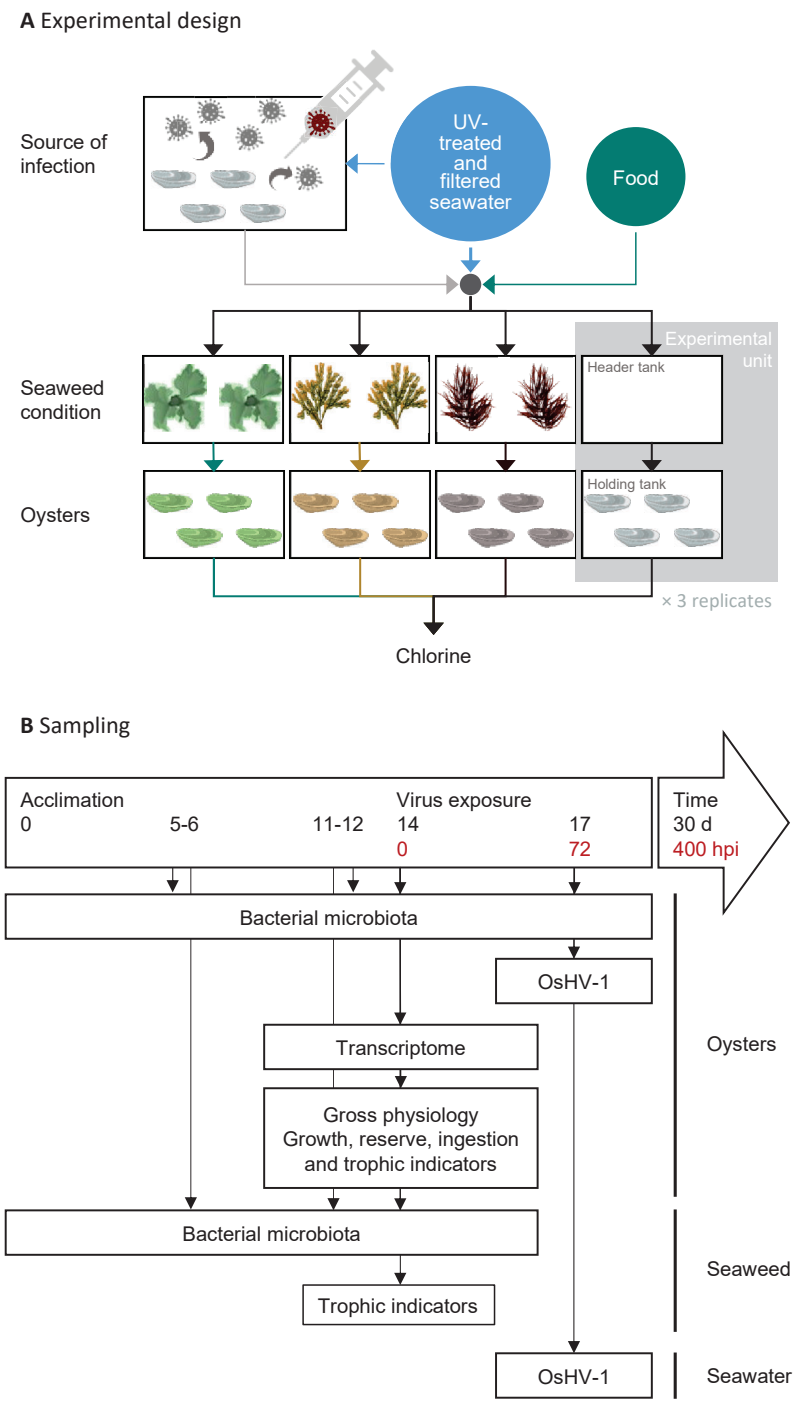
A Experimental design
Source of infection
UV-treated and filtered seawater
Food
Seaweed condition
Oysters
Header tank
Holding tank
Experimental unit
× 3 replicates
Chlorine
B Sampling
Acclimation
0
5-6
11-12
Virus exposure
14
0
17
72
Time
30 d
400 hpi
Bacterial microbiota
OsHV-1
Transcriptome
Gross physiology
Growth, reserve, ingestion
and trophic indicators
Oysters
Bacterial microbiota
Trophic indicators
Seaweed
OsHV-1
Seawater

Fig. 1

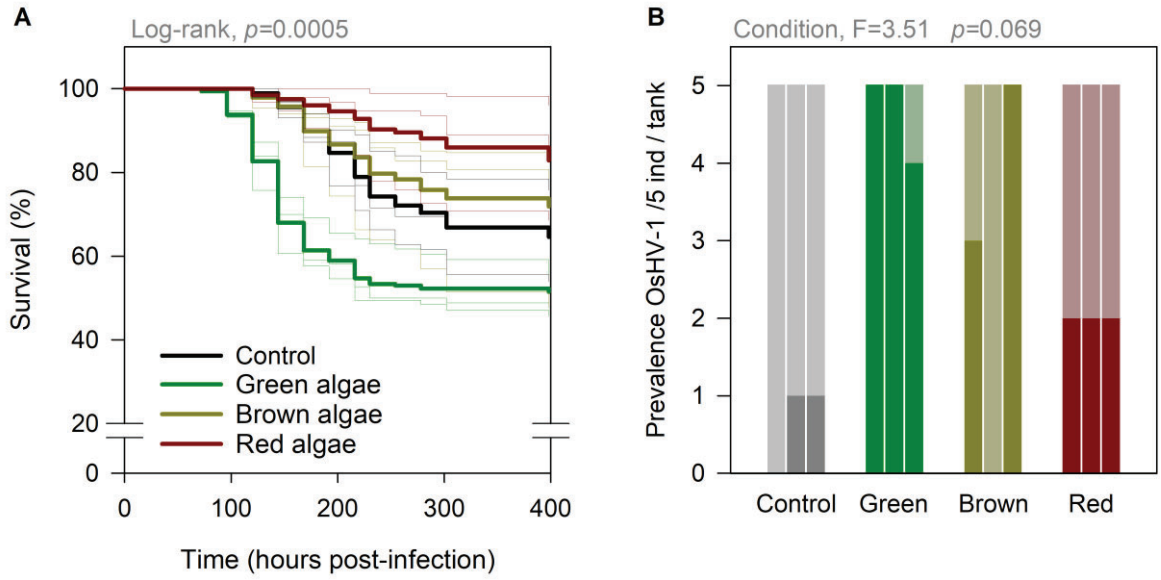
A
Log-rank, p=0.0005
Survival (%)
100
80
60
40
20
0
0
100
200
300
400
Time (hours post-infection)
Control
Green algae
Brown algae
Red algae
B
Condition, F=3.51 p=0.069
Prevalence OsHV-1 /5 ind / tank
5
4
3
2
1
0
Control
Green
Brown
Red

Fig. 2.

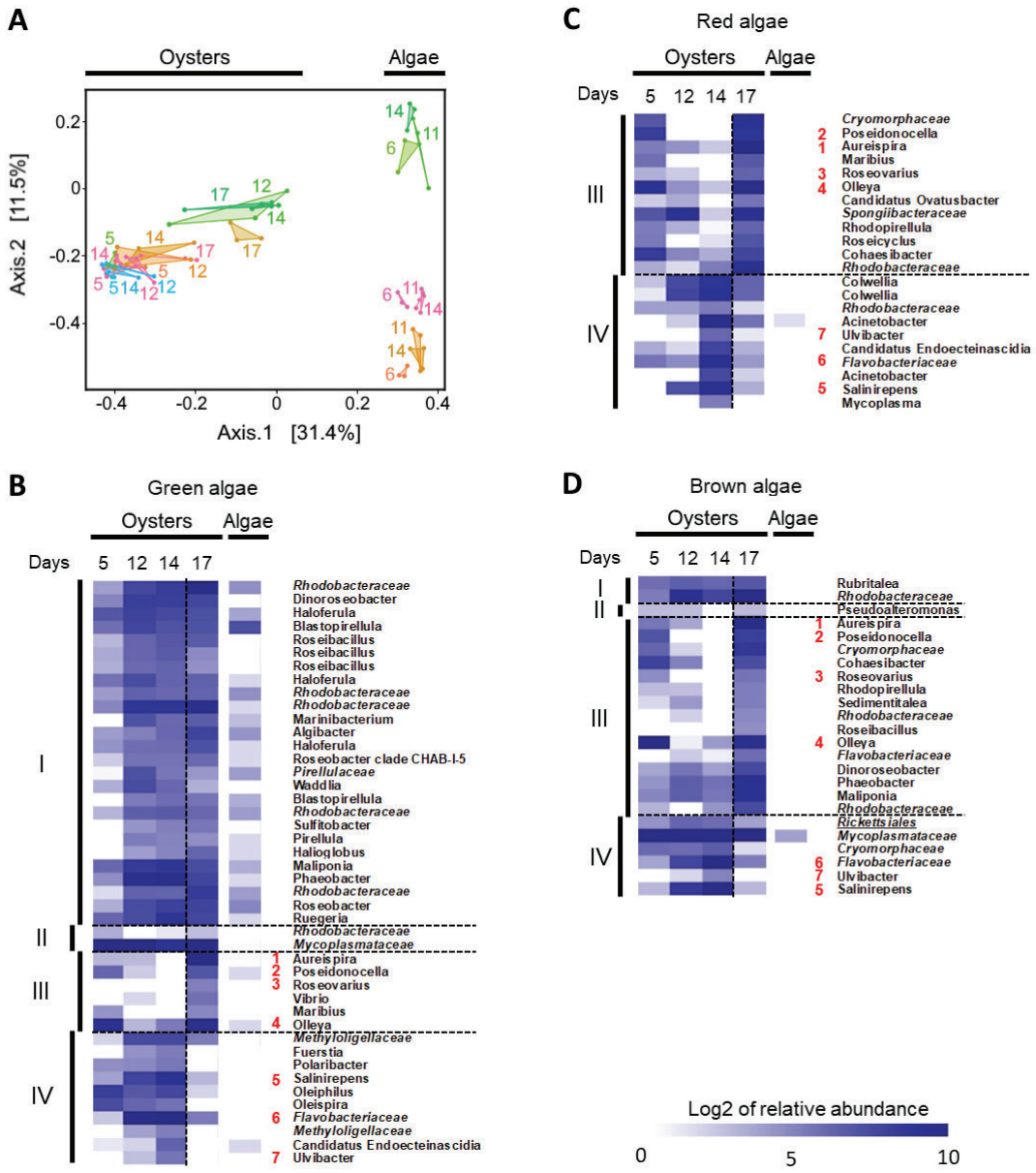
A
Oysters
Algae
Axis.2 [11.5%]
Axis.1 [31.4%]
B
Green algae
Oysters
Algae
Days 5 12 14 17
I
II
III
IV
Rhodobacteraceae
Dinoroseobacter
Haloferula
Blastopirellula
Roseibacillus
Roseibacillus
Roseibacillus
Haloferula
Rhodobacteraceae
Rhodobacteraceae
Marinibacterium
Algibacter
Haloferula
Roseobacter clade CHAB-I-5
Pirellulaceae
Waddlia
Blastopirellula
Rhodobacteraceae
Sulfitobacter
Pirellula
Halioglobus
Maliponia
Phaeobacter
Rhodobacteraceae
Roseobacter
Ruegeria
Rhodobacteraceae
Mycoplasmataceae
1 Aureispira
2 Poseidonocella
3 Roseovarius
Vibrio
Maribius
4 Olleya
Methyloligellaceae
Fuerstia
Polaribacter
5 Salinirepens
Oleiphilus
Oleispira
6 Flavobacteriaceae
Methyloligellaceae
Candidatus Endoecteinascidia
7 Ulvibacter
C
Red algae
Oysters
Algae
Days 5 12 14 17
III
IV
Cryomorphaceae
2 Poseidonocella
1 Aureispira
Maribius
3 Roseovarius
4 Olleya
Candidatus Ovatusbacter
Spongiibacteraceae
Rhodopirellula
Roseicyclus
Cohaesibacter
Rhodobacteraceae
Colwellia
Colwellia
Rhodobacteraceae
Acinetobacter
7 Ulvibacter
Candidatus Endoecteinascidia
6 Flavobacteriaceae
Acinetobacter
5 Salinirepens
Mycoplasma
D
Brown algae
Oysters
Algae
Days 5 12 14 17
I
II
III
IV
Rubritalea
Rhodobacteraceae
Pseudoalteromonas
1 Aureispira
2 Poseidonocella
Cryomorphaceae
Cohaesibacter
3 Roseovarius
Rhodopirellula
Sedimentitalea
Rhodobacteraceae
Roseibacillus
4 Olleya
Flavobacteriaceae
Dinoroseobacter
Phaeobacter
Maliponia
Rhodobacteraceae
Ricketts iales
Mycoplasmataceae
Cryomorphaceae
6 Flavobacteriaceae
7 Ulvibacter
5 Salinirepens
Log2 of relative abundance
0
5
10

Fig. 3.

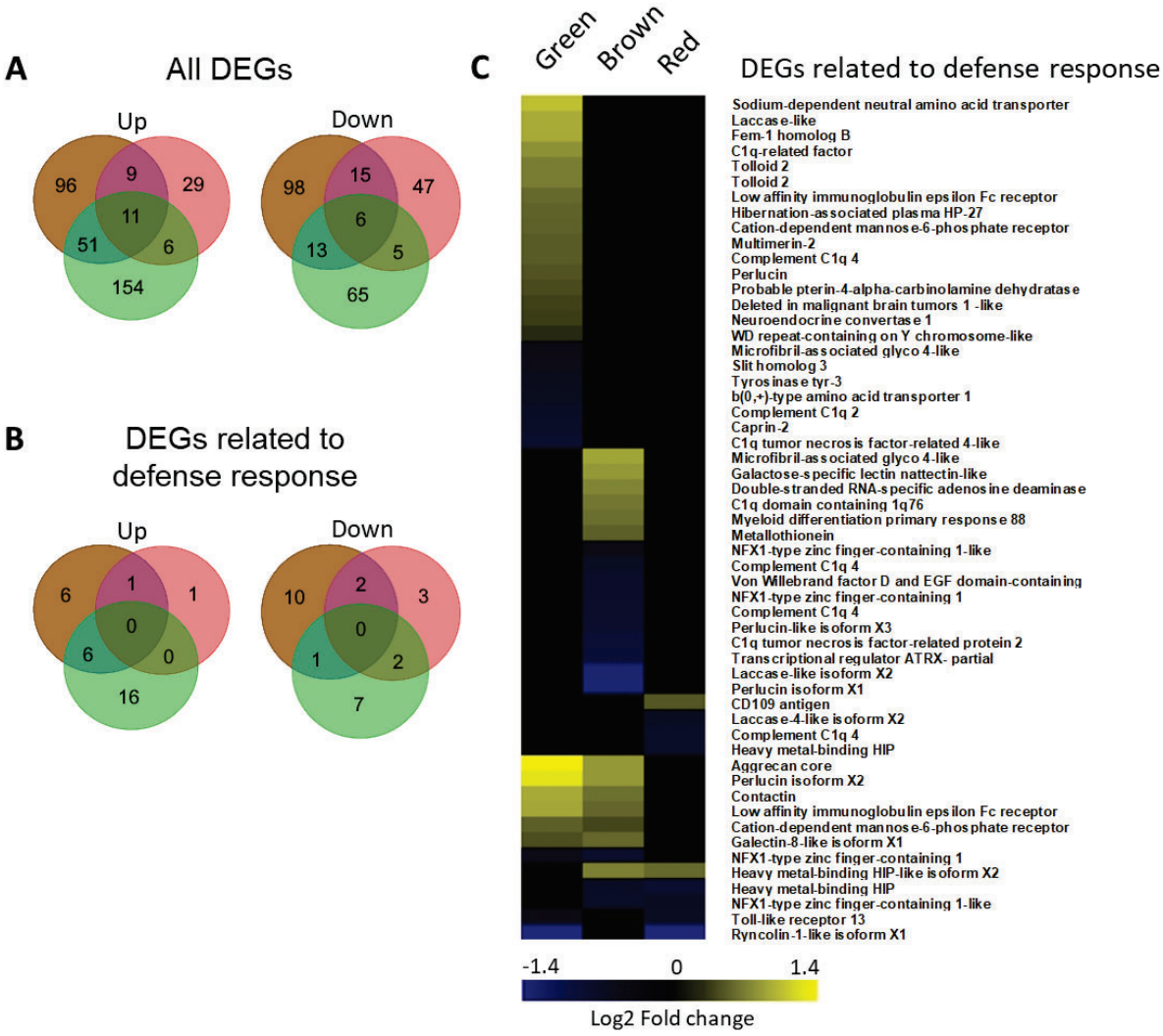
A
All DEGs
Up
Down
96
9
29
11
51
6
154
98
15
47
6
13
5
65
B
DEGs related to defense response
Up
Down
6
1
1
0
6
0
16
10
2
3
0
1
2
7
C
Green
Brown
Red
DEGs related to defense response
Sodium-dependent neutral amino acid transporter
Laccase-like
Fem-1 homolog B
C1q-related factor
Tolloid 2
Tolloid 2
Low affinity immunoglobulin epsilon Fc receptor
Hibernation-associated plasma HP-27
Cation-dependent mannose-6-phosphate receptor
Multimerin-2
Complement C1q 4
Perlucin
Probable pterin-4-alpha-carbinolamine dehydratase
Deleted in malignant brain tumors 1 -like
Neuroendocrine convertase 1
WD repeat-containing on Y chromosome-like
Microfibril-associated glyco 4-like
Slit homolog 3
Tyrosinase tyr-3
b(0,+)-type amino acid transporter 1
Complement C1q 2
Caprin-2
C1q tumor necrosis factor-related 4-like
Microfibril-associated glyco 4-like
Galactose-specific lectin nattectin-like
Double-stranded RNA-specific adenosine deaminase
C1q domain containing 1q76
Myeloid differentiation primary response 88
Metallothionein
NFX1-type zinc finger-containing 1-like
Complement C1q 4
Von Willebrand factor D and EGF domain-containing
NFX1-type zinc finger-containing 1
Complement C1q 4
Perlucin-like isoform X3
C1q tumor necrosis factor-related protein 2
Transcriptional regulator ATRX- partial
Laccase-like isoform X2
Perlucin isoform X1
CD109 antigen
Laccase-4-like isoform X2
Complement C1q 4
Heavy metal-binding HIP
Aggrecan core
Perlucin isoform X2
Contactin
Low affinity immunoglobulin epsilon Fc receptor
Cation-dependent mannose-6-phosphate receptor
Galectin-8-like isoform X1
NFX1-type zinc finger-containing 1
Heavy metal-binding HIP-like isoform X2
Heavy metal-binding HIP
NFX1-type zinc finger-containing 1-like
Toll-like receptor 13
Ryncolin-1-like isoform X1
-1.4
0
1.4
Log2 Fold change

Fig. 4.